An update on QCD+QED simulations with C* boundary conditions

Conference Paper

Author(s):
Bushnaq, Lucius; Campos, Isabel; Catillo, Marco; Cotellucci, Alessandro; Dale, Madeleine; Fritzsch, Patrick; Lücke, Jens; Marinkovic, Marina ⓘD; Patella, Agostino; Tantalo, Nazario

An update on QCD+QED simulations with C⋆ boundary conditions

Lucius Bushnaq,[a] **Isabel Campos,**[b] **Marco Catillo,**[c] **Alessandro Cotellucci,**[d] **Madeleine Dale,**[ef] **Patrick Fritzsch,**[a] **Jens Lücke,**[dg,*] **Marina Krstić Marinković,**[c] **Agostino Patella**[dg] **and Nazario Tantalo**[ef]

[a]*School of Mathematics, Trinity College Dublin, Dublin 2, Ireland*

[b]*Instituto de Física de Cantabria & IFCA-CSIC, Avda. de Los Castros s/n, 39005 Santander, Spain*

[c]*Institut für Theoretische Physik, ETH Zürich, Wolfgang-Pauli-Str. 27, 8093 Zürich, Switzerland*

[d]*Humboldt Universität zu Berlin, Institut für Physik & IRIS Adlershof, Zum Großen Windkanal 6, 12489 Berlin, Germany*

[e]*Università di Roma Tor Vergata, Dip. di Fisica, Via della Ricerca Scientifica 1, 00133 Rome, Italy*

[f]*INFN, Sezione di Tor Vergata, Via della Ricerca Scientifica 1, 00133 Rome, Italy*

[g]*DESY, Platanenallee 6, D-15738 Zeuthen, Germany*

E-mail: jens.luecke@hu-berlin.de, agostino.patella@physik.hu-berlin.de, fritzscp@tcd.ie, isabel.campos@csic.es, bushnaql@tcd.ie, m.dale@stimulate-ejd.eu, nazario.tantalo@roma2.infn.it, mcatillo@ethz.ch, marinama@phys.ethz.ch, alessandro.cotellucci@physik.hu-berlin.de

RC⋆QR collaboration

We present two novelties in our analysis of fully dynamical QCD+QED ensembles with C⋆ boundary conditions. The first one is the explicit computation of the sign of the Pfaffian. We present an algorithm that provides a significant speedup compared to traditional methods. The second one is a reweighting of the mass in the context of the RHMC. We have tested the techniques on both pure QCD and QCD+QED ensembles with pions at $m_{\pi^{\pm}} \approx 400$ MeV, a lattice spacing of $a \approx 0.05$ fm, a fine-structure constant of $\alpha_R = 0$ and 0.04.

The 38th International Symposium on Lattice Field Theory, LATTICE2021 26th-30th July, 2021
Zoom/Gather@Massachusetts Institute of Technology

---

*Speaker

1. Introduction

We present an update on a long-term research program aiming at calculating isospin-breaking and QED radiative corrections in hadronic quantities, with C⋆ boundary conditions [1–4] and fully-dynamical QCD+QED simulations. C⋆ boundary conditions allow for a local and gauge-invariant formulation of QED in finite volume and in the charged sector of the theory [5–7]. In particular, two ensembles were generated at the values of the fine-structure constant $\alpha_R = 0.04$ and $\alpha_R = 0$. A value of α_R larger than the physical one has been chosen to amplify QED corrections.

The open-source openQ*D-1.1 code [8, 9] was used to generate all gauge configurations presented in this work. This code has been developed by the RC⋆ collaboration. It is an extension of the openQCD-1.6 code [10] for QCD.

In this proceedings we will focus on two novelties in our analysis: the calculation of the sign of the Pfaffian of the Dirac operator (section 3), and a particular implementation of the mass reweighting in the context of the RHMC (section 4).

2. Simulation setup

So far we have generated two $N_f = 3 + 1$ QCD ensembles and two $N_f = 1 + 2 + 1$ QCD+QED ensembles. We used the Lüscher-Weisz action for the SU(3) field with $\beta = 3.24$, the Wilson action for the U(1) field with $\alpha_0 = 0.05$ (for the QCD+QED ensembles), and $O(a)$-improved Wilson fermions. For the QCD ensembles, we used the value of c_{sw} determined non-perturbatively in [11]. For the QCD+QED ensembles, in lack for a better option, we used the same value of c_{sw} for the SU(3) SW term, and $c_{sw} = 1$ for the U(1) SW term (see table 1). We employ C⋆ boundary conditions in space and periodic boundary conditions in time for all our ensembles. We have verified that we are free from the problem of topological freezing in all our ensembles, which justifies the use of periodic boundary conditions in time.

Following [12], we determine the lattice spacing from the auxiliary observable t_0, by using the central value of the CLS determination $(8t_0)^{1/2} = 0.415$ fm [13]. This has been taken only as an indicative value, keeping in mind that it contains an $O(\alpha_0)$ ambiguity which can be resolved only when the scale is set with a physical observable, e.g. the mass of the Ω baryon. We obtain $a \simeq 0.054$ fm for the QCD ensembles, and a marginally lower value for the QCD+QED ensembles (see table 2).

We define the renormalized fine-structure constant α_R as

$$\alpha_R = \mathcal{N}^{-1} t_0^2 \langle E_{U(1)}(t_0) \rangle \tag{1}$$

where $E_{U(1)}(t)$ is the clover discretization of the U(1) action density calculated in terms of the gauge field at positive flow time t. The normalization $\mathcal{N}$ is chosen such that $\alpha_R = \alpha_0 + O(\alpha_0^2)$. Our choice $\alpha_0 = 0.05$ for the QCD+QED ensembles, corresponds to an unphysically large value $\alpha_R \simeq 0.04 \simeq 5.5 \alpha_R^{phys}$.

In the QCD case, we have simulated the SU(3) symmetric point, i.e. $m_u = m_d = m_s \simeq (m_u + m_d + m_s)^{phys}/3$. In the QCD+QED case, we have chosen to work at the U-symmetric point, i.e. $m_d = m_s$, and we have chosen m_u in such a way that the strong isospin-breaking effects are
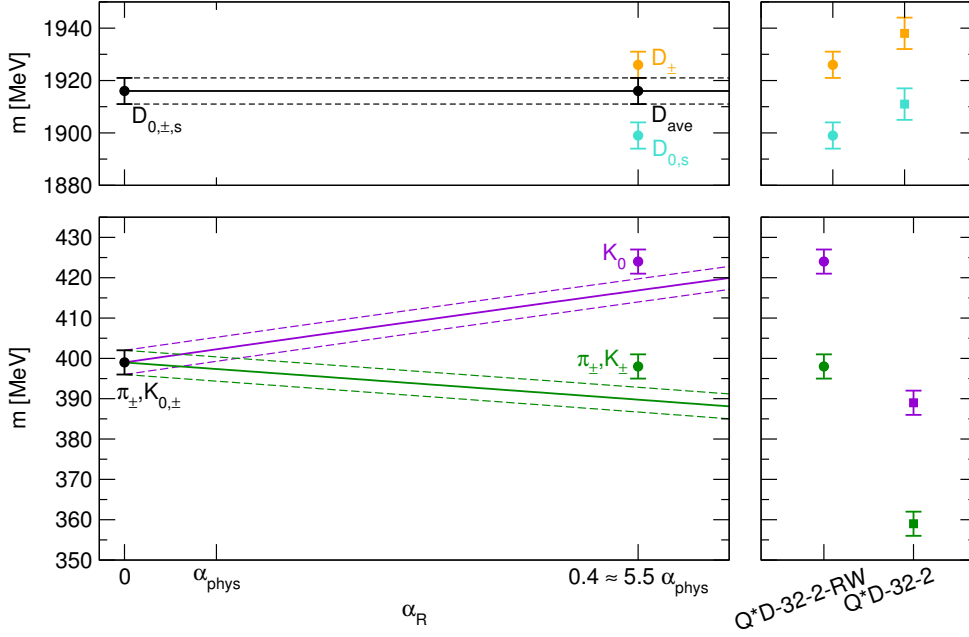
Figure 1: Lines of constant physics. The black points on the left correspond to the ensemble `QCD-32-1`. The π and the K mass that we measured served as starting points to set our lines of constant physics. Following the lines on the right one can see the masses measured on the `Q*D-32-2-RW` ensemble. While the average of the D-mesons is perfectly on the line of constant physics, the kaons are slightly too heavy. The plot on the right visualizes the shift that we managed to achieve with the reweighting.

rescaled with the same factor as the QED isospin-breaking effects. The *lines of constant physics* are determined by keeping the following quantities

$$\phi_0 = 8t_0(m_{K^\pm}^2 - m_{\pi^\pm}^2) , \qquad \phi_1 = 8t_0(m_{\pi^\pm}^2 + m_{K^\pm}^2 + m_{K^0}^2) ,$$
$$\phi_2 = 8t_0(m_{K^0}^2 - m_{K^\pm}^2)\alpha_R^{-1} , \qquad \phi_3 = \sqrt{8t_0}(m_{D_s} + m_{D^0} + m_{D^\pm}) , \qquad (2)$$

constant as α is varied. While these quantities can be determined quite accurately from lattice simulations, their real-world value is unknown, since t_0 cannot be measured experimentally. In practice one needs to simulate different lines of constant physics, and then interpolate/extrapolate to the real-world one by setting the scale with a physical observable. The aim of this project is to simulate on the U-symmetric line of constant physics defined by

$$\phi_0 = 0 , \quad \phi_1 = 2.13 \simeq \phi_1^{\text{phys}} , \quad \phi_2 = 2.37 \simeq \phi_2^{\text{phys}} , \quad \phi_3 = 12.1 \simeq \phi_3^{\text{phys}} , \qquad (3)$$

which, for $\alpha = 0$, corresponds to the QCD SU(3)-symmetric point. In this setup the $\pi^\pm$ is heavier than the real-world one, making simulations easier. In the context of QCD+QED, a similar strategy has been used e.g. in [14]. As routinely done in QCD (and more so in the past), one wants to start from heavier pions and then to approach the physical pion mass in steps.

The most important parameters and observables for our ensembles have been summarized in tables 2, 3, 4. In these tables we include also the run `Q*D-32-2+RW` which is obtained by reweighting the `Q*D-32-2` ensemble in the bare quark masses (chosen in such a way to hit the target tuning point). The values of the ϕ_i that we measured can be seen in table 4. The resulting lines of constant physics can be seen in figure 1.

ensemble	α	κ_u	$\kappa_d = \kappa_s$	κ_c	$c_{\text{sw,SU(3)}}$	$c_{\text{sw,U(1)}}$
QCD-32-1	0	0.13440733	0.13440733	0.12784	2.18859	0
Q*D-32-1	0.05	0.135479	0.134524	0.12965	2.18859	1
Q*D-32-2	0.05	0.135560	0.134617	0.129583	2.18859	1
Q*D-32-2+RW	0.05	0.1355368	0.134596	0.12959326	2.18859	1

Table 1: Simulation parameters. For the first three ensembles, the hopping parameters $\kappa_{u,d,s,c}$ are the ones actually used to generate the configurations. For Q*D-32-2+RW, the values of $\kappa_{u,d,s,c}$ are the ones used in the reweighting procedure.

ensemble	volume	cnfgs	a	α_R	L	$m_{\pi^\pm}L$
QCD-32-1	64×32^3	2000	0.0539(3) fm	0	1.73(1) fm	3.49(3)
Q*D-32-1	64×32^3	1993	0.0526(2) fm	0.04077(6)	1.682(5) fm	4.18(2)
Q*D-32-2	64×32^3	2001	0.0505(3) fm	0.04063(6)	1.62(1) fm	2.90(3)
Q*D-32-2+RW	64×32^3	2001	0.0510(2) fm	0.0407(1)	1.631(6) fm	3.24(3)

Table 2: *cnfg* stands for the number of thermalized configurations for the first three ensembles, or number of reweighted configurations for Q*D-32-2+RW. The lattice spacing a is calculated by assuming $\sqrt{8t_0} = 0.415$ fm with no error. L is the linear size of the spatial box. The results are preliminary.

ensemble	$m_{\pi^\pm} = m_{K^\pm}$	$m_{K^0} - m_{K^\pm}$	$m_{D^0} = m_{D_s}$	$m_{D^\pm} - m_{D^0}$	$\pi\sqrt{3}L^{-1}$
QCD-32-1	399(3) MeV	0 MeV	1916(5) MeV	0 MeV	—
Q*D-32-1	495(3) MeV	23.3(5) MeV	1871(6) MeV	32(1) MeV	639(2) MeV
Q*D-32-2	359(3) MeV	30(1) MeV	1911(6) MeV	26(2) MeV	664(4) MeV
Q*D-32-2+RW	398(3) MeV	26(1) MeV	1899(5) MeV	27(2) MeV	658(3) MeV

Table 3: Summary of masses. The masses for charged hadrons have been corrected for the universal $O(\alpha_R)$ finite-volume corrections. The quantity $\pi\sqrt{3}L^{-1}$ is the smallest energy of a free photon in the considered finite box with C* boundary conditions in all directions. The results are preliminary.

ensemble	ϕ_1	ϕ_2	ϕ_3
QCD-32-1	2.11(3)	—	12.09(3)
Q*D-32-1	3.36(4)	2.56(5)	11.93(4)
Q*D-32-2	1.81(3)	2.4(1)	12.16(5)
Q*D-32-2+RW	2.20(3)	2.32(8)	12.09(3)

Table 4: Summary of tuning observables. All ensembles are at the U-symmetric point, i.e. $m_d = m_s$ or $\phi_0 = 0$. The $\phi_{0,1,2,3}$ are described in the main text. Our main goal was to tune the QCD+QED parameters in such a way that $\phi_{1,3}$ are equal to the QCD runs, while $\phi_2 = \phi_2^{\text{phys}} \simeq 2.37$. The results are preliminary.

3. Sign of the Pfaffian

Given a quark field ψ, we introduce the corresponding antiquark field $\psi^C = C^{-1}\bar{\psi}^T$, where the charge-conjugation matrix C can be chosen to be $i\gamma_0\gamma_2$ in the chiral basis. C⋆ boundary conditions for the fermion fields can be written as

$$\begin{pmatrix} \psi(x + L\hat{k}) \\ \psi^C(x + L\hat{k}) \end{pmatrix} = \begin{pmatrix} \psi^C(x) \\ \psi(x) \end{pmatrix} \equiv T \begin{pmatrix} \psi(x) \\ \psi^C(x) \end{pmatrix} . \tag{4}$$

With C⋆ boundary conditions the Dirac operator D acts on the quark-antiquark doublet in a non-diagonal way, and it is therefore a $24V \times 24V$ matrix. The integration of a quark field in the path integral yields the Pfaffian pf $[CTD]$ in place of the standard fermionic determinant. We rewrite the Pfaffian as

$$\text{pf}\,[CTD] = W_{\text{sgn}}\,|\text{pf}\,[CTD]| = W_{\text{sgn}}\,|\det[D]|^{1/2} \,, \tag{5}$$

where we have used the algebraic relation pf $[M]^2 = \det[M]$ for a general antisymmetric matrix M. In practice we treat the sign W_{sgn} of the Pfaffian as a reweighing factor. In previous work we have left this out because close to the continuum one expects $W_{\text{sgn}} \simeq 1$.

In order to calculate its sign, it is convenient to relate the Pfaffian to the spectrum of the hermitian Dirac operator $Q = \gamma_5 D$. We first observe that the spectrum of Q is doubly degenerate: if v is an eigenvector of Q, then one easily checks that $CT\gamma_5 v^*$ is also an eigenvector of Q with same eigenvalue, and the two eigenvectors are orthogonal. Let $\lambda_{n=1,\ldots,12V} \in \mathbb{R}$ be the list of eigenvalues of Q, each of them appearing a number of times equal to half their degeneracy. Then one proves that

$$\text{pf}\,[CTD]^2 = \det[D] = \det[Q] = \prod_{n=1}^{12V} \lambda_n^2 \,, \qquad\qquad \text{pf}\,[CTD] = \prod_{n=1}^{12V} \lambda_n \,. \tag{6}$$

While the first relation is trivial, the second relation follows from the fact that both sides of the equation are analytic functions of the bare mass m_0, and they diverge to $+\infty$ in the $m_0 \to +\infty$ limit. It follows that the Pfaffian is positive (resp. negative) if the number of negative eigenvalues λ_n is even (resp. odd). In practice we calculate the sign by following the eigenvalue flow as a function of m_0. At very large mass, Q is approximately equal to $m_0\gamma_5$ and the number of negative eigenvalues is even. As m_0 is decreased towards its target value, the Pfaffian flips sign every time an eigenvalue of Q crosses zero. In practice, we follow the flow in the opposite direction, increasing m_0 until a crossing becomes unlikely.

Our method is based on two steps: (A) a first fast algorithm identifies a small subset of configurations for which a potential crossing may occur, (B) on these configurations we apply the methods described in [15, 16] to determine whether a crossing actually occurs.[1] We describe here only the step A, which is the truly novel ingredient in our calculation.

Let $\bar{\lambda}$ be the smallest eigenvalue of the operator $|Q|$, i.e.

$$\bar{\lambda} = \min_n |\lambda_n| \,. \tag{7}$$

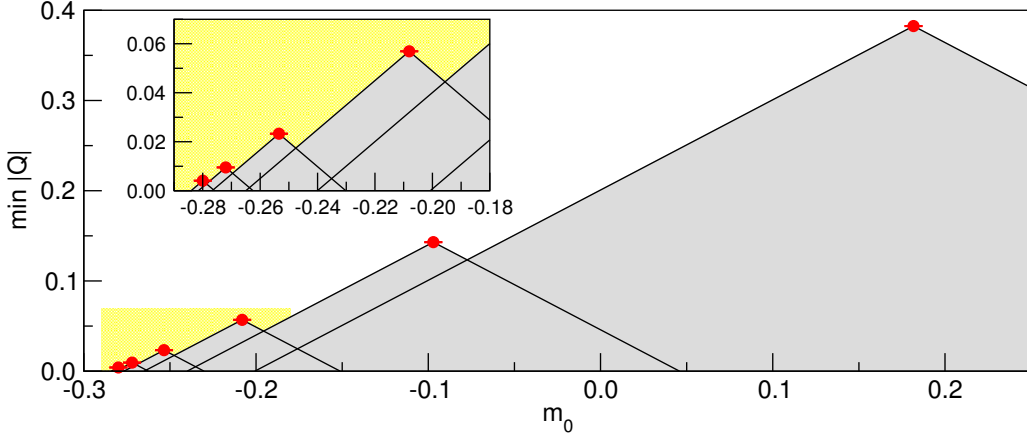[1]An alternative method has been proposed in [17].

Figure 2: Smallest eigenvalue of $|Q|$ as a function of the valence mass m_0 (red points), calculated on a representative configuration (QCD-32-1 ensemble). Using the bound on the derivative (8), one proves that no eigenvalue of $|Q|$ can flow in the grey areas. In particular, no eigenvalue crosses zero in the explored range of masses. One can see that we are able to flow the eigenvalue across two orders of magnitude in only six steps. As evident from the plot an even more efficient version of the algorithm would skip every other step. The inset is a zoom-in of the yellow area.

Since $Q'(m_0) = \gamma_5$, using the Feynman-Hellmann theorem one proves that the derivative of *every* eigenvalue of $Q(m_0)$ satisfies the hard bound

$$\left|\lambda'_n(m_0)\right| = |(\psi_n, Q'(m_0)\psi_n)| = |(\psi_n, \gamma_5\psi_n)| \le 1 . \tag{8}$$

It easily follows that, if $\bar{\lambda}(m_0) > 0$, then no eigenvalue of $Q(\tilde{m}_0)$ crosses zero for $m_0 - \bar{\lambda}(m_0) < \tilde{m}_0 < m_0 + \bar{\lambda}(m_0)$. This observation allows to design the following algorithm, to be run on each configuration:

1. Set $m_0^{(0)} = m_0$ and $n = 0$.
2. Calculate $\bar{\lambda}^{(n)} = \bar{\lambda}(m_0^{(n)})$.
3. If $n \ge 1$ and $\bar{\lambda}^{(n)} < \bar{\lambda}^{(n-1)}$ then stop the algorithm and apply step B.
4. If $m_0^{(n)} > m_0^{\max}$ then stop the algorithm and set $W_{\text{sgn}} = 1$.
5. Define $m_0^{(n+1)} = m_0^{(n)} + c\bar{\lambda}^{(n)}$ and repeat from point 2 with $n \leftarrow n + 1$.

The number c could be 2 if we were able to calculate the eigenvalue with infinite precision, but it is chosen to be slightly smaller than 2 for safety. The scan in mass terminates either when the eigenvalue decreases or when the arbitrarily chosen maximal mass $m_0^{\max}$ is reached. In most configurations the eigenvalue does not decrease, which implies that the increment in m_0 increases at every iteration. In a few iterations, one can easily cover a couple of orders of magnitude in the eigenvalue $\bar{\lambda}$, as illustrated in figure 2. We stress that in this step we do not need to track eigenvectors, but only the smallest eigenvalue of $|Q|$, which can be efficiently and reliably calculated by applying the power method plus Chebyshev's acceleration to the operator Q^{-2}.

None of the generated ensembles showed a negative sign after the Markov chain thermalized. During thermalization however, some gauge field configurations were present with a negative Pfaffian. One such example from a QCD+QED ensemble can be seen in figure 3.
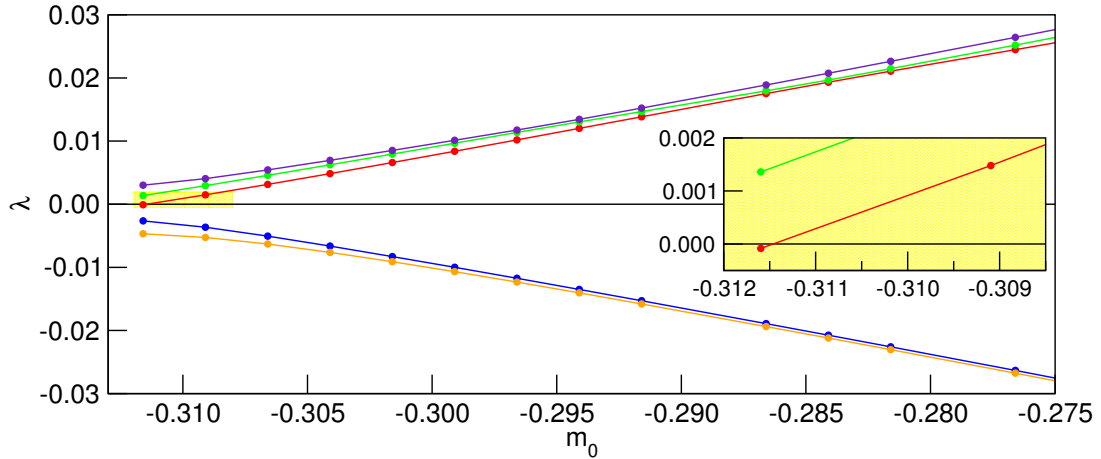
Figure 3: Mass flow for the up quark. We see that for larger bare masses m_0 the gap of the Dirac operator Q increases. However between the first and the second measurement the red eigenvalue flows across zero and induces a sign flip of the Pfaffian. This sign was observed on a configuration before the Markov chain thermalized. Hence in the final analysis it did not enter. The inset is a zoom-in of the yellow area.

4. Reweighting of the mass

In figure 1 one can see that, for the `Q*D-32-2` ensemble, both kaons are roughly 40 MeV too light and the average of the D-mesons is around 10 MeV too heavy. To correct these mistunings we use a reweighting in the mass [18].[2] We represent the absolute value of the fermionic Pfaffian as in

$$\left|\mathrm{pf}\left[CTD_m\right]\right| = \left|\det\left[D_m\right]\right|^{1/2} = \frac{\left|\det\left[D_m^{\mathrm{oo}}\right]\right|^{1/2}}{\det\left[\hat{Q}_m^2\right]^{-1/4}} \rightarrow \frac{\left|\det\left[D_m^{\mathrm{oo}}\right]\right|^{1/2}}{\det\left[R(\hat{Q}_m^2)\right]} \ . \tag{9}$$

Here $\hat{Q}_m$ is defined as $\gamma_5 \hat{D}_m$ where $\hat{D}_m$ is the even-odd preconditioned Dirac operator, while D_m^{oo} is the Dirac operator restricted to and projected onto the odd sites. The operator $(\hat{Q}_m^2)^{-1/4}$ is replaced by a rational approximation $R(\hat{Q}_m^2)$, whose inverse determinant is stochastically estimated by introducing pseudofermion fields in a standard fashion (for more details see [9]). We choose a rational approximation R of order (n, n) of the form

$$R\left(\hat{Q}_m^2\right) = A \prod_{i=1}^{n} \frac{\hat{Q}_m^2 + \nu_i^2}{\hat{Q}_m^2 + \mu_i^2} \ . \tag{10}$$

The parameters are chosen such that R is the optimal rational approximation on a given interval $[r_a, r_b]$, in the sense that the uniform relative error is minimized.

So for a reweighting of the mass one needs two factors[3]

$$W_{\mathrm{mass}} = \det\left[R\left(\hat{Q}_m^2\right) R^{-1}\left(\hat{Q}_{m'}^2\right)\right], \qquad W_{\mathrm{eo}} = \left|\det\left[D_{m'}^{\mathrm{oo}}(D_m^{\mathrm{oo}})^{-1}\right]\right|^{1/2} \ . \tag{11}$$

---

[2]An algorithm for one-flavour mass reweighting has been proposed in [19], however this algorithm does not apply to the case of $C^\star$ boundary conditions since the fermionic determinant is replaced by the Pfaffian.

[3]The two rational approximations in W_{mass} can be different. This is useful if the spectral range of the approximated operator changes significantly.

The W_{eo} factor is only present with even-odd preconditioning and is calculated exactly. The factor W_{mass} can be written as a product of determinants of positive hermitian operators

$$W_{\text{mass}} = \prod_{j=1}^{2n} \det \left[\left(1 + \delta\hat{D}S_j\right)^{\dagger} \left(1 + \delta\hat{D}S_j\right) \right] \ . \tag{12}$$

The difference of the Dirac operators $\delta\hat{D} = \hat{D}_{m'} - \hat{D}_m$ can be worked out analytically. The operator S_j is defined as

$$S_j = \left(\hat{D}_m + i\gamma_5\nu_j\right)^{-1} - \left(\hat{D}_{m'} + i\gamma_5\mu_j\right)^{-1} - \left(\hat{D}_{m'} + i\gamma_5\mu_j\right)^{-1} \delta\hat{D} \left(\hat{D}_m + i\gamma_5\nu_j\right)^{-1} \ . \tag{13}$$

In practice, every determinant from eq. (12) is estimated stochastically, i.e.

$$W_{\text{mass}} = \prod_{j=1}^{2n} \det \left[1 + R_j \right] = \prod_{j=1}^{2n} \left(\frac{1}{N_j} \sum_{l=1}^{N_j} e^{-\left(\eta_{jl}, R_j \eta_{jl}\right)} \right) \ . \tag{14}$$

The hermitian operator R_j is defined as

$$R_j = \left(\delta\hat{D}S_j\right)^{\dagger} + \left(\delta\hat{D}S_j\right) + \left(\delta\hat{D}S_j\right)^{\dagger} \left(\delta\hat{D}S_j\right) \ , \tag{15}$$

and the complex stochastic sources η have support on the even lattice sites and a probability distribution proportional to $e^{-(\eta,\eta)}$.

We computed the reweighting factor with a single stochastic source for every factor. Investigating the effects of the reweighting shows that in our case the mistuning was small enough, so that we do not observe an increase in the errors. In the tables 3 and 4 this can be seen explicitly. The reweighting induces a slight shift in the lattice spacing, but within errors the electromagnetic coupling stayed the same. From table 2 one can see that only ϕ_1 is off the line of constant physics after reweighting.

5. Summary

For the first time we have computed the sign of the Pfaffian and included it into our analysis. Thus we are simulating the full path integral. We have presented a two-part algorithm that can efficiently detect gauge field configurations that give a negative fermionic Pfaffian. For our ensembles we did not observe any configurations with negative sign once the Markov chain thermalized. It will be interesting to see at which pion masses and what lattice spacings negative signs actually become a problem.

After the reweighting in the mass, no significant increase in the error of any observable was observed. For a larger shift and larger volumes we expect an increase in the errors. A preliminary analysis showed that the computation of the mass reweighting factor is about 40% cheaper than the generation of a new ensemble without considering thermalization. Since the tuning of the parameters in a fully dynamical QCD+QED simulation is a complex task and in practice requires the generation of several tuning ensembles, it is interesting in what regime of quark masses and for what volumes the reweighting gives reasonable results.

References

[1] A. S. Kronfeld and U. J. Wiese, Nucl. Phys. B **357** (1991), 521-533

[2] A. S. Kronfeld and U. J. Wiese, Nucl. Phys. B **401** (1993), 190-205 [arXiv:hep-lat/9210008].

[3] U. J. Wiese, Nucl. Phys. B **375** (1992), 45-66

[4] L. Polley, Z. Phys. C **59** (1993), 105-108

[5] B. Lucini, A. Patella, A. Ramos and N. Tantalo, JHEP **02** (2016), 076 [arXiv:1509.01636].

[6] A. Patella, PoS **LATTICE2016** (2017), 020 [arXiv:1702.03857].

[7] M. Hansen, B. Lucini, A. Patella and N. Tantalo, JHEP **05** (2018), 146 [arXiv:1802.05474].

[8] (RC*), I. Campos, P. Fritzsch, M. Hansen, M. Krstić Marinković, A. Patella, A. Ramos et al., "openQ*D." GitLab: https://gitlab.com/rcstar/openQxD. CSIC: https://dx.doi.org/10.20350/digitalCSIC/8591, https://hdl.handle.net/10261/173334.

[9] I. Campos *et al.* [RC*], Eur. Phys. J. C **80** (2020) no.3, 195 [arXiv:1908.11673].

[10] *Simulation program for lattice QCD (openQCD code)*, https://cern.ch/luscher/openQCD, 2016.

[11] P. Fritzsch *et al.* [ALPHA], JHEP **06** (2018), 025 [erratum: JHEP **10** (2020), 165] [arXiv:1805.01661].

[12] R. Höllwieser, F. Knechtli and T. Korzec, PoS **LATTICE2019** (2019), 025 [arXiv:1907.04309].

[13] M. Bruno, T. Korzec and S. Schaefer, Phys. Rev. D **95** (2017) no.7, 074504 [arXiv:1608.08900].

[14] R. Horsley, Y. Nakamura, H. Perlt, D. Pleiter, P. E. L. Rakow, G. Schierholz, A. Schiller, R. Stokes, H. Stüben and R. D. Young, *et al.* J. Phys. G **43** (2016) no.10, 10LT02 [arXiv:1508.06401].

[15] I. Campos *et al.* [DESY-Munster], Eur. Phys. J. C **11** (1999), 507-527 [arXiv:hep-lat/9903014].

[16] D. Mohler and S. Schaefer, Phys. Rev. D **102** (2020) no.7, 074506 [arXiv:2003.13359].

[17] G. Bergner and J. Wuilloud, Comput. Phys. Commun. **183** (2012), 299-304 [arXiv:1104.1363].

[18] A. Hasenfratz, R. Hoffmann and S. Schaefer, Phys. Rev. D **78** (2008), 014515 [arXiv:0805.2369].

[19] J. Finkenrath, F. Knechtli and B. Leder, Nucl. Phys. B **877** (2013), 441-456 [erratum: Nucl. Phys. B **880** (2014), 574-575] [arXiv:1306.3962].